Annals of Biomedical Engineering, Vol. 48, No. 8, August 2020 (© 2020) pp. 2192–2203
https://doi.org/10.1007/s10439-020-02561-6

Original Article

Matrix Deformation with Ectopic Cells Induced by Rotational Motion in Bioengineered Neural Tissues

NICOLAS ROULEAU,[1,2,3] NIROSHA J. MURUGAN,[1,3,4] WILLIAM RUSK,[1] COLE KOESTER,[1] and DAVID L. KAPLAN[1,2,3]

[1]Department of Biomedical Engineering, Science & Technology Center, Tufts University, Medford, MA, USA; [2]Initiative for Neural Science, Disease, and Engineering (INSciDE), Tufts University, Medford, USA; [3]The Allen Discovery Center, Tufts University, Medford, USA; and [4]Department of Biology, Tufts University, Medford, USA

(*Received 21 March 2020; accepted 29 June 2020; published online 15 July 2020*)

Associate Editor Leonidas D. Iasemidis oversaw the review of this article.

Abstract—The brain's extracellular matrix (ECM) is a dynamic protein-based scaffold within which neural networks can form, self-maintain, and re-model. When the brain incurs injuries, microscopic tissue tears and active ECM remodelling give way to abnormal brain structure and function including the presence of ectopic cells. Post-mortem and neuroimaging data suggest that the brains of jet pilots and astronauts, who are exposed to rotational forces, accelerations, and microgravity, display brain anomalies which could be indicative of a mechanodisruptive pathology. Here we present a model of non-impact-based brain injury induced by matrix deformation following mechanical shaking. Using a bioengineered 3D neural tissue platform, we designed a repetitive shaking paradigm to simulate subtle rotational acceleration. Our results indicate shaking induced ectopic cell clustering that could be inhibited by physically restraining tissue movement. Imaging revealed that the collagen substrate surrounding cells was deformed following shaking. Applied to neonatal rat brains, shaking induced deformation of extracellular spaces within the cerebral cortices and reduced the number of cell bodies at higher accelerations. We hypothesize that ECM deformation may represent a more significant role in brain injury progression than previously assumed and that the present model system contributes to its understanding as a phenomenon.

Keywords—Tissue engineering, Extracellular matrix, Microtearing, Ectopic cells, Cortical neurons.

ABBREVIATIONS

ECM	Extracellular matrix
rpm	Revolutions per minute
DAPI	4′,6-Diamidino-2-phenylindole
CA	Calcein-AM
PI	Propidium iodide
WBV	Whole-body vibrations

INTRODUCTION

Brains change radically over the course of normal development and maturation. From neurogenesis,[34] to embryonic tissue patterning,[27] post-natal synaptic pruning[26] and life-long remodeling associated with memory encoding and consolidation,[23] it is evident that the structure of the brain is fundamentally dynamic. The brain's capacity to re-model itself has also been observed following traumatic injury,[10] stroke,[41] and other insults.[11] Because the regenerative capacities of the brain are limited,[14] post-injury re-modelling is not fully restorative and can even contribute to abnormal electrophysiological changes[15] and tissue degeneration.[12] Indeed, it has become increasingly apparent that injury-induced microtearing[17,25] and subsequent active re-modelling[35] of the extracellular matrices (ECM)—the delicate connective tissues that provide neurons and glia with complex scaffolding through which dense networks are formed—are disruptive to the integrity of neural tissue function. This is perhaps unsurprising as ectopic neurons can be

Address correspondence to David L. Kaplan, Department of Biomedical Engineering, Science & Technology Center, Tufts University, Medford, MA, USA. Electronic mail: david.kaplan@tufts.edu

0090-6964/20/0800-2192/0 © 2020 Biomedical Engineering Society

observed following injury events,[30] suggesting a weakening of ECM-cell interactions. With brain structure, balance is critical—too little capacity for change and processes such as synaptogenesis would not be possible. Too much change, however, would threaten the constancy of normal function including the maintenance of higher-order cognitive features including personality and the fidelity of memory.

Though it is conventionally assumed that an impact event is necessary to initiate brain trauma cascades, a growing body of literature suggests otherwise. Whole-body vibration (WBV) has been a long suspected cause of intracranial injury in humans[31] and some authors have even speculated that WBV may be linked to neural degeneration.[24] Indeed, animal models of WBV produced by motor vehicles caused diffuse, microscopic brain lesions.[39,40] Similarly, rotational acceleration has been considered a source of non-impact-based brain injury associated with activities such as machining, the use of jackhammers, and off-road vehicles.[18] It is therefore relevant to consider non-impact mechanodisruption of brain structure as part of an extended spectrum of brain-perturbing influences.

Idiopathic and often asymptomatic white matter hyperintensities (WMHs) have been detected within the brains of jet pilots and astronauts [1,20]—special populations that are exposed to vibrations,[3] acceleration forces, and microgravity environments. It has been assumed that deep-brain WMHs detected with T2-weighted magnetic resonance imaging (MRI) and fluid attenuated inversion recovery (FLAIR) sequences indicate the presence of lacunes and other vascular pathologies. However, similar signal hyperintensities can be caused by any vacuolation of brain space. Indeed, analyses of post-mortem brain tissues suggest that the source of WMHs are heterogeneous; they can be made up of tissues characterized by gliosis, loosening white matter, demyelination, as well as protein aggregation and are typically periventricular.[38] Some authors have suggested that asymptomatic WMHs in jet pilots could be indicative of cumulative brain damage.[21] Models of non-impact-based brain mechanodisruption are therefore important to pursue in an age marked by increased efforts to commercialize space travel.

Brains exhibit remarkable mechanical properties including viscoelasticity, deforming temporarily under transient stress and permanently under maintained stress.[13] Upon mechanical impact, brains elongate, compress, and shear within the skull over the course of milliseconds—radically changing network and cellular ultrastructure. However, it is unknown how brains respond to more subtle mechanical perturbations including vibration and rotational acceleration without impact. Just as shear waves can propagate through human brain tissues with complex, frequency-dependent transmission, interacting preferentially with certain structures,[6,8] there may be equivalent effects associated with other non-impact-based mechanical events. Here, we present a model of brain tissue disruption using varied rotational forces to explore their effects on tissue integrity.

Three-dimensional tissue culture models using novel biomaterials represent powerful alternatives to classical, monolayer-based tissue culture and offer a relatively high-throughput solution to the challenges of studying the effects of brain injury in controlled settings.[32] Bioengineered tissue models allow researchers to work between *in vivo* and *in vitro* contexts. We have previously designed and fabricated custom neural tissues to simulate both rodent[7] and human[4,5] cortices using neurons and glia as well as silk protein as a bioscaffold.[34] Based upon previous demonstrations of cell-ECM interactions associated with brain injury,[9] we designed paradigms to examine the effects of subtle mechanical perturbations on tissue integrity. We conclude that matrix deformation and subsequent tissue disorganization was caused by the mechanical shaking paradigm and discuss its potential implications.

METHODS

3D Cell Culture

Bioengineered neural tissues were assembled following our previously published protocol.[7] Briefly, embryonic rat (Sprague-Dawley, Taconic) cortical cells were harvested from E18 pups and seeded in scaffolds composed of silk fibroin (6% w/v) with 500–600 μm pores that were previously coated in poly-D-lysine (0.1 mg/mL) to facilitate cell attachment. The Tufts University Institutional Animal Care and Use Committee (IACUC) approved all procedures involving animals according to NIH guidelines. Each scaffold was injected with a 100 μL aliquot of media containing 10^6 cells within individual wells of an uncoated 96-well culture plate. The media formulation consists of Gibco Neurobasal medium (Thermo Fisher), 1% v/v GlutaMAX Supplement (Thermo Fisher), 2% v/v B27 supplement (Thermo Fisher), and 1% v/v penicillin–streptomycin (Corning). After the 24-h seeding incubation period (37 °C, 5% CO[15,27] 5% relative humidity) to ensure cell attachment, scaffolds were moved to new wells and embedded in 7.4 pH-adjusted (NaOH) collagen type-I (rat tail, 3 mg/mL) hydrogel to simulate brain ECM. Plates were incubated for 30 min before adding 100 μL of fresh medium and returned to the incubator to stabilize the gel overnight. The next

day, scaffolds were transferred to 24-well plates using micro-forceps where they remained submerged in 1 mL of medium for long-term maintenance. Half of the media was replaced every 3 days. A 2-week period of growth and maturation was enforced before cells were exposed to any experimental conditions. Each sample consisted of a 6 mm (diameter) by 2 mm (height) cylindrical silk sponge with a 2 mm core or window within its central volume. The central windows, devoid of cell bodies, were perfused with collagen gel (i.e., hydrogel with no silk fibers) and served as spaces within which neurites could be extended to form connections across the tissue constructs.

3D MECHANICAL SHAKING PARADIGM

To simulate a rotational, acceleration-based injury, a mechanical shaking paradigm was designed which involved continuously shaking tissues for brief periods over the course of several days. Tissue culture plates containing cells within individual wells were removed from the incubator and placed on a Compact Digital MicroPlate Shaker (Thermo Fisher Scientific, US) at room temperature (23 °C). The shaking platform was set to counterclockwise motion (the default setting of the device) and the angular velocity was set to between 150 and 270 revolutions per minute (rpm), initiated, and terminated after 10 min of continuous exposure (Fig. 1). The range of angular velocities was selected such that the minimum (150 rpm) represented the lowest possible setting and the maximum (270 rpm) represented the upper-bound level beyond which media would escape the well due to rotational forces. For 3D experiments, samples displayed a complex profile of motion consisting of counterclockwise rotation within their respective wells with jerking, counterclockwise epicycles (Fig. 1). To control for effects of temperature, environment, and manipulation, plates were placed directly adjacent to the orbital shaker to accommodate variance between conditions explained by time outside of the incubator (e.g., temperature, handling). This procedure was repeated daily for 5 consecutive days. All samples remained in their maintenance wells in 24-well plates during exposure though a subset of samples were transferred to trans-well inserts (6 mm diameter, 24-well insert) before each exposure and re-submerged in media. Trans-well inserts (Fig. 1) were used to immobilize the samples within their individual wells, minimizing free movement around the base of the well (i.e., inhibiting epicycle motion). To control for physical manipulation effects (e.g., use of forceps), some 3D samples were transferred to trans-wells without exposure to the orbital shaker (i.e., manipulated but not shaken).

2D CELL CULTURE FOLLOWING SUBSTRATE DEFORMATION

We hypothesized that the localized structure and concentration of the collagen substrate would determine how cells would become organized within the scaffold and that repeated deformation in 3D would generate anisotropies across the matrix. To verify whether microscopic tears or hyperdensities could be generated in our ECM conditions, monolayers (2D cell culture) of primary cortical cells (isolated from E18 animals) were seeded within 24-well plates on top of pre-disrupted (shaken) gel matrices (Fig. 1). One day before cell isolation and seeding, wells were filled with 1 mm-thick collagen gels (3 mg/mL type-I rat collagen, pH-adjusted to 7.4). After 30 min of incubation to solidify the gel, 1 mL of Dulbecco's phosphate-buffered saline (DPBS) was added to each well to maintain hydration. Then, plated substrates were exposed to mechanical perturbations: 50 min of continuous shaking (1 day only). Differences between the 3D and 2D paradigms are due to intrinsic limitations of viability associated with monolayers under repetitive non-incubation conditions. After disruption, cells were seeded on top of the collagen substrates at a density of 1.8×10^5 cells/cm^2 and maintained in supplemented neurobasal medium as described previously. It was necessary to mechanically perturb the gel substrates before plating cells to parse the order of events within the causal chain; without pre-exposing the substrate to mechanical shaking, it would not be possible to know whether increased angular velocities were mobilizing cells which in turn modified their surrounding matrices or if the ECM was being deformed independently, affecting cells in turn.

Live/Dead Staining: Viability Imaging

Living cells were imaged following a 15 min incubation (37 °C) in 1 mL DPBS containing 8 μM of the cell-permeant dye, Calcein AM (CA; Invitrogen, Thermo Fisher Scientific) diluted in DMSO (1 mg/mL). Dead cells were stained with 10 μM propidium iodide (PI; Thermo Fisher). CA (ex: 490 nm, em: 515 nm) and PI (ex: 535 nm, em: 617 nm) fluorescence, indicative of live and dead cells respectively, were captured using a Nikon Eclipse Ti2 Inverted Microscope System (FITC, DAPI, and TRITC Filter Cubes) with a Zyla 5.5 sCMOS (Andor) side-mounted camera. To visualize cells distributed throughout 3D samples, 100 μm (z-stack) maximum projection images were captured, focused, and subjected to background subtraction using the constant method in NIS-Elements. Monochromatic data were transformed to RGB values in ImageJ (1.47v).

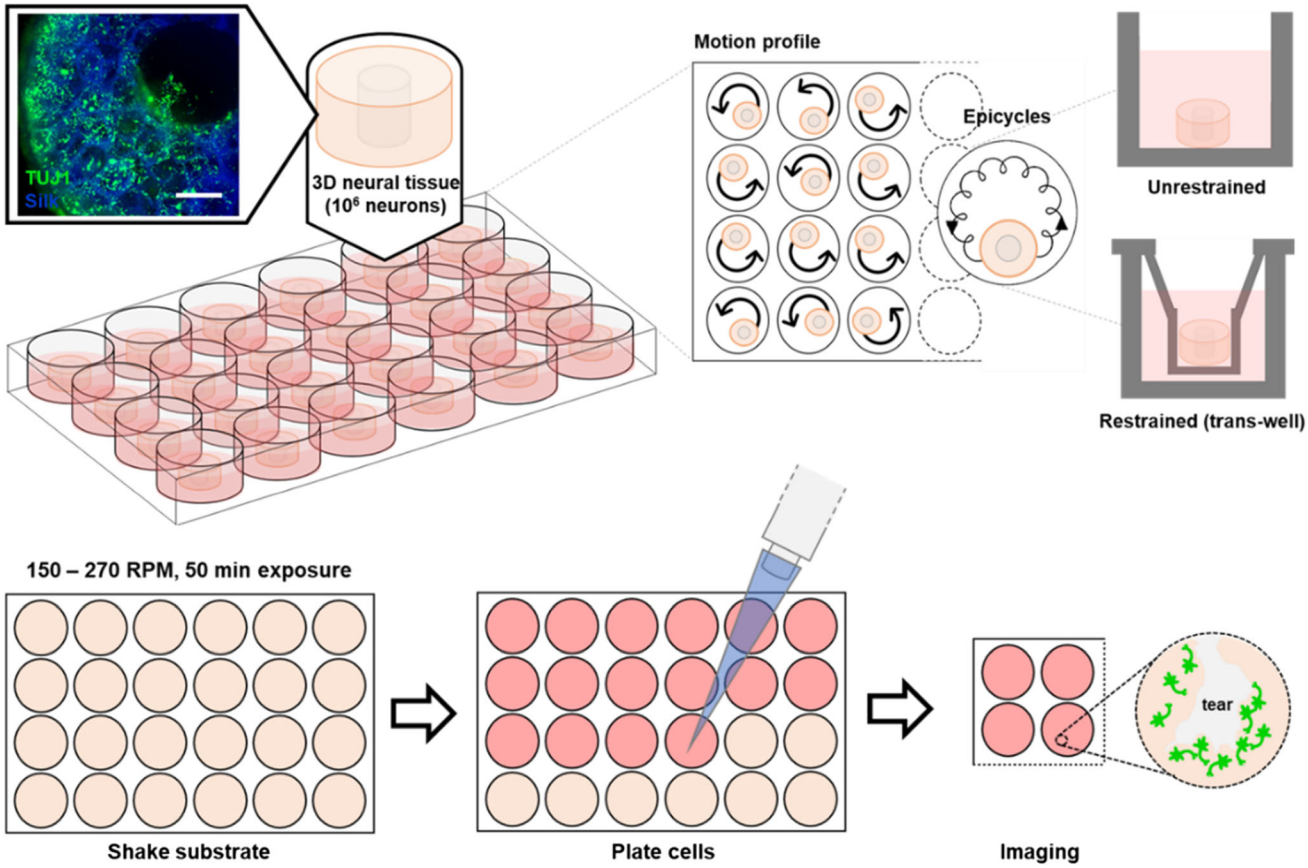

FIGURE 1. The mechanical shaking paradigm. (Top row) 3D bioengineered neural tissue samples comprised of silk scaffolds (blue, Silk) seeded with primary rat cortical neurons (green, TUJ1) were loaded into 24-well plates with media. The plates were shaken with static angular velocities between 150 and 270 rpm for 10 min per day for 5 days; the motion profile of samples within wells was counterclockwise with notable epicycles. Some samples were restrained with trans-well inserts to impede motion. (Bottom row) 2D Collagen substrates were pre-shaken for 50 min and cells were subsequently plated on top of the perturbed gels. Imaging was performed to examine the effects of substrate structure on cellular organization.

Densiometry: Reflectance Imaging

As the mechanical shaking paradigm was suspected to affect hydrogel structure within the central window of each 3D culture sample, silk scaffolds were embedded in collagen type-I as described previously though without the addition of cells. Samples containing no cells will herein be referred to as "blank" samples. In addition to the standard, low-concentration (3 mg/mL) collagen gels, some silk scaffolds were embedded in high-concentration (6 mg/mL) collagen hydrogels. Once exposed to the mechanical shaking paradigm (10 min/exposure, 5 days of exposure), blank samples were subjected to a densiometric imaging protocol. Using the Leica TCS SP8 Confocal Microscope system, a 552 nm fluorescent laser was directed through the construct while reading between 545 and 555 nm with the tunable PMT. Areas of increased density were inferred based upon increased reflectance, detected as increased signal within the PMT wavelength sampling band. Areas of spatially continuous, increased reflectance relative to background were designated as "collagen islands". These regions were identified by generating thresholds of increased fluorescence in ImageJ (1.47v), converting them to 8-bit binary images, and using the Analyze Particles function to identify independent objects within the field of view. If the hydrogel was uniformly dense, few islands would be identified; however, as the local density became more spatially variable, more islands would become apparent.

Mechanical Disruption of Neonatal Rat Brains

To demonstrate the relevance of the applied forces associated with the mechanical shaking paradigm on brain ECM, full rodent brains (*ex vivo*) were exposed to a limited range of angular velocities on orbital shakers: No shaking, 150 rpm (low-intensity), or 270 rpm (high-intensity). We reasoned that although the mechanical shaking paradigm is not necessarily analogous to a particular exposure which might be

encountered in everyday life, it would still be necessary to demonstrate that the applied forces could realistically impact native brain structure. Following IACUC-approved methods of euthanasia (CO_2 and decapitation), neonatal rat brains (P1) were surgically removed from pups and placed in 1 mL of supplemented neurobasal medium in 24-well plates. Brains were exposed to 50 min of shaking at room temperature immediately following excision. It was not possible to expose neonatal brains to multiple days of shaking as we aimed to minimize the role of post-mortem decay on ECM deformation. Upon completion of the mechanical exposure, brains were chemically fixed in 4% paraformaldehyde (PFA) in phosphate buffered saline (PBS) for subsequent processing and histology.

Immunocytochemistry: 3D Neural Tissues

All bioengineered samples were first fixed in 4% PFA in PBS for 30 min. After fixation, samples were washed with DPBS several times and immersed in a blocking solution (20 mg/mL bovine serum albumin, 2% (v/v) donkey serum, and 0.2% (v/v) Triton X-100 in DPBS) for 1 h. Once the samples were blocked, a 1:1000 dilution of the primary antibody solution—mouse anti-βIII Tubulin antibody (TUJ1, Thermo Fisher Scientific) and rabbit anti-glial fibrillary protein, (GFAP, Thermo Fisher Scientific)—was added to the 1.5 mL of blocking solution and cultures were incubated at 4 °C for 24 h to permit perfusion. Subsequent to primary antibody incubation, samples were washed several times with DPBS and exposed to diluted (1:250) secondary antibodies conjugated to fluorophores (Alexa Fluor™ 488 and 647, Thermo Fisher Scientific) for 24 h. The next day, samples were washed with DPBS, incubated at room temperature for 5 min in a 300 nM solution of 4′,6-diamidino-2-phenylindole (DAPI) in DPBS, followed by another wash period and maintained in DPBS long-term at 4 °C. Fluorescent imaging was performed within 1 week of staining. Images were acquired using a Leica TCS SP8 Confocal Microscope with fluorescence capabilities. Photomultiplier tubes (PMTs) with tunable bandwidth filters (spectral range 400–800 nm) were used to track emission spectra associated with fluorophore excitation. *Z*-stacks consisting of 200 μm sections were constructed using maximum projection images.

Immunohistochemistry: Neonatal Rat Brain ECM

Immunohistochemical detection of ECM deformation was performed following neonatal rat brain exposure to the mechanical shaking paradigm. Once exposed and fixed, full neonatal brains were cryoprotected with increasing concentrations of sucrose (10 to 30%) and embedded in optimal cutting temperature compound (OCT). Each brain was partitioned into 14 μm coronal sections using a Leica CM1850 Cryostat. Immunohistochemistry was then performed, targeting chondroitin sulfate (CS)—a major component of the proteoglycan-rich neural ECM. The same staining protocol as outlined previously was used; however, the primary antibody was a monoclonal anti-CS species made in mice (Sigma-Aldrich) diluted to 1:1000. The secondary antibody was an anti-mouse Alexa Fluor™ 488 diluted to 1:250. DAPI was applied during the mounting step (DAPI Fluoromount-G, Thermo Fisher). Only a subset of sections proximal to a fixed reference point (Interaural 6.00 mm, Bregma -3.00 mm) which displayed both dorsal hippocampal bodies (HB) and primary somatosensory cortices (S1) were analyzed. These stereotaxic coordinates were selected for their central position along the neuraxis[37] and the target regions, HB and S1, were selected to represent both superficial and deep structures. Images were acquired using the Nikon Eclipse Ti2 Inverted Microscope System and processed in ImageJ (1.47v). Mean gray values (MGV) were computed for fluorescent signals (CS-positive and DAPI-positive) across the CA fields of the HB and within layers I–V of S1. Before measuring MGV, fluorescent images were processed by conversion to 8-bit format and conversion to binary images.

Statistical Analysis

All statistical analyses were performed in IBM SPSS version 20. Assumptions of normality were tested before the use of parametric testing including ANOVAs, *t*-tests, and correlational analyses (Pearson's *r*). Significant differences were assumed if *p* values were below a threshold of 0.05 (two-tailed hypothesis testing).

RESULTS

Ectopic Clustering of Cell Bodies Following Mechanical Shaking

Examining the central windows of tissue samples exposed to the mechanical shaking paradigm, an interaction between angular velocity and restraint conditions on the presence of DAPI-positive signal (cell bodies) was observed, $F(6,45) = 3.76$, $p = 0.01$, $\eta^2 = 0.20$ (Figs. 2b and 2c). When examining cases associated with the use of trans-well inserts, no significant effect of angular velocity was noted ($p > 0.05$). However, when left unrestrained, angular velocity significantly impacted the presence of DAPI-

positive signal within the central window, $F(6,24) = 4.24$, $p < 0.01$, $\eta^2 = 0.59$. The major source of variance was a difference between non-shaken coAntrol samples and those which were exposed to an angular velocity of 220 rpm, $t(4) = 4.49$, $p < 0.01$, explaining 83% of the variance. A similar effect was observed when comparing samples exposed to 150 and 220 rpm, $t(4) = 4.42$, $p < 0.01$, $r^2 = 0.83$. Indeed, only after increasing the angular velocity to 170 rpm did samples begin to display the presence of ectopic cells within the central window. When left undisturbed (not shaken), cell bodies were rarely observed within the central window and remained confined to the silk-rich regions at the periphery of the construct. A limited set of trials were conducted to determine whether a single 10 min exposure to 220 rpm shaking was sufficient to induce ectopic clustering; the same effect was evident ($p < 0.05$, data not shown), suggesting even a brief mechanical exposure could affect the distribution of cells throughout the sample.

To determine whether clustered cells could continue to live within the central window following mechanical exposures, samples were stained with a cell-permeant dye, Calcein-AM, and imaged. Fluorescent images revealed clustered live cell populations scattered throughout the hydrogel when shaking matched or exceeded angular velocities of 170 rpm (Fig. 2c). Fragmented collagen windows containing ~ 150 μm-wide clusters were observed; cells displayed a particular affinity for the edges of collagen films that had lifted from the bulk hydrogel mass (Figs. 2c and 2d). Indeed, when physically perturbed during imaging, these structures and their attached cells would visibly oscillate within the aqueous environment. For samples exposed to mild shaking (150 rpm) or control conditions (no shaking), live cells remained confined to the silk scaffold regions. These data indicated that sufficiently high-intensity shaking induced live cells to cluster within the central window and that when physically restrained, clustering was prevented.

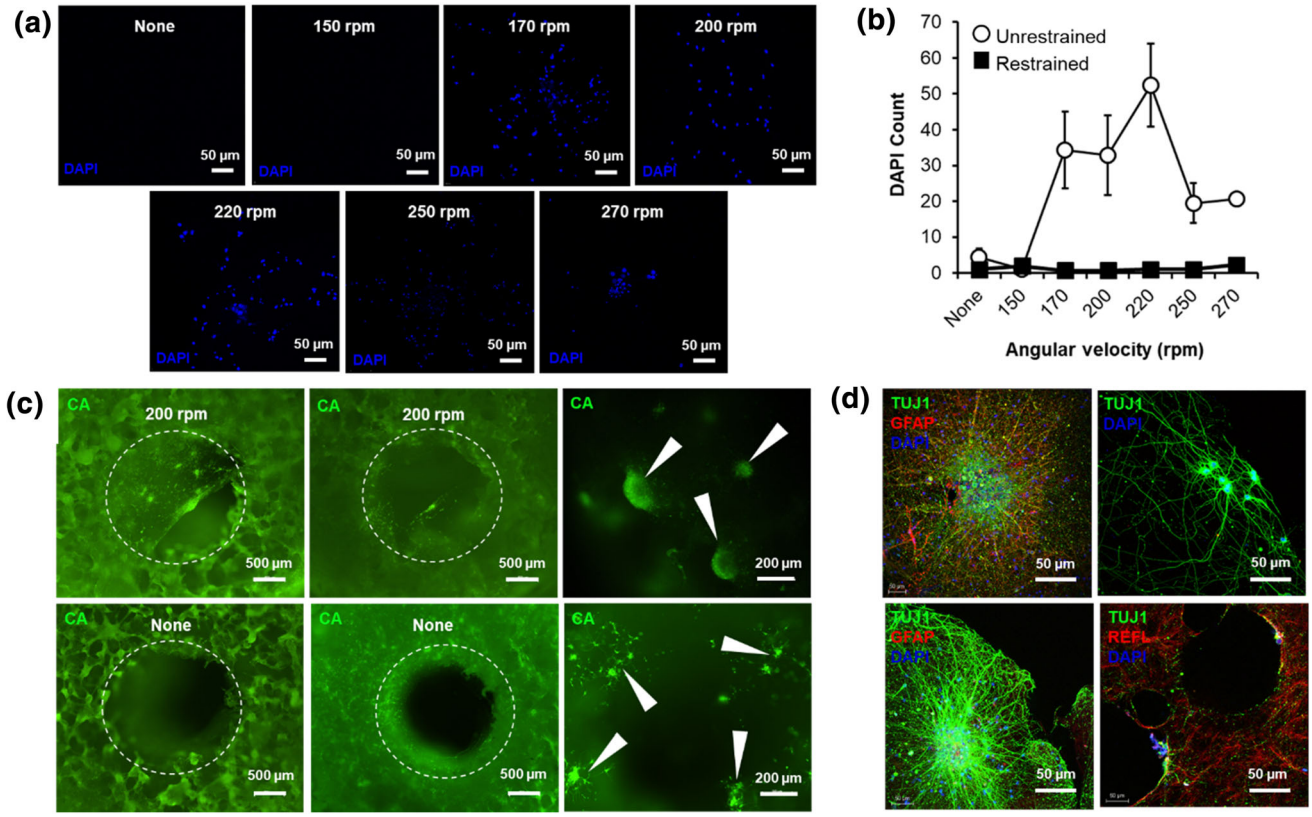

FIGURE 2. Living ectopic cell clusters within the central collagen window following mechanical shaking. DAPI-positive cell bodies (a, blue) display non-linear clustering patterns following mechanical shaking (b, open circles) with increased angular velocity which are attenuated by physical restraint using trans-well inserts (b, closed squares). Cells expressing CA-positive signal indicate that newly formed clusters within the central collagen windows (c, dashed circle) continue to live after 5 days of exposure to the mechanical shaking paradigm. White arrows indicate clusters at higher magnification (c). Immunocytochemistry revealed fine processes including dendritic arbors (d, TUJ1, green) remained intact with some glial presence within clusters (d, GFAP, red). Cells could be found clinging to the edges of collagen structures as indicated by simultaneous reflectance (d, REFL, red) imaging. Means and standard error of the means are presented. All scale bars are indicated.

Collagen Hydrogel Deformation Following Mechanical Shaking

The impact of angular velocity and collagen concentration on the formation of collagen islands, regions of increased optical density, within blank (no cells) scaffolds was assessed, revealing a significant interaction, $F(6,52) = 5.12$, $p < 0.001$, $\eta^2 = 0.16$. Among blank samples containing low concentration collagen (3 mg/mL), angular velocity impacted collagen island formation non-linearly (Figs. 3a, 3b and 3c). The major sources of variance were significantly increased collagen islands within blank samples exposed to 200 and 220 rpm relative to non-shaken controls ($p < 0.001$) and the 150 rpm condition ($p < 0.001$). Interestingly, 250 and 270 rpm conditions did not generate more collagen islands relative to controls ($p > 0.05$). Next, blank samples containing high concentration collagen (6 mg/mL) were examined and it was evident that more collagen islands could be discerned in non-shaken controls relative to the equivalent blank samples from the low concentration condition, $t(4) = 4.26$, $p < 0.05$. Nevertheless, angular velocity impacted collagen island formation among high concentration samples as well, where the 200 rpm condition continued to generate more islands when compared to the non-shaken control condition ($p < 0.001$). The impact of angular velocity on collagen island formation remained non-linear for blank

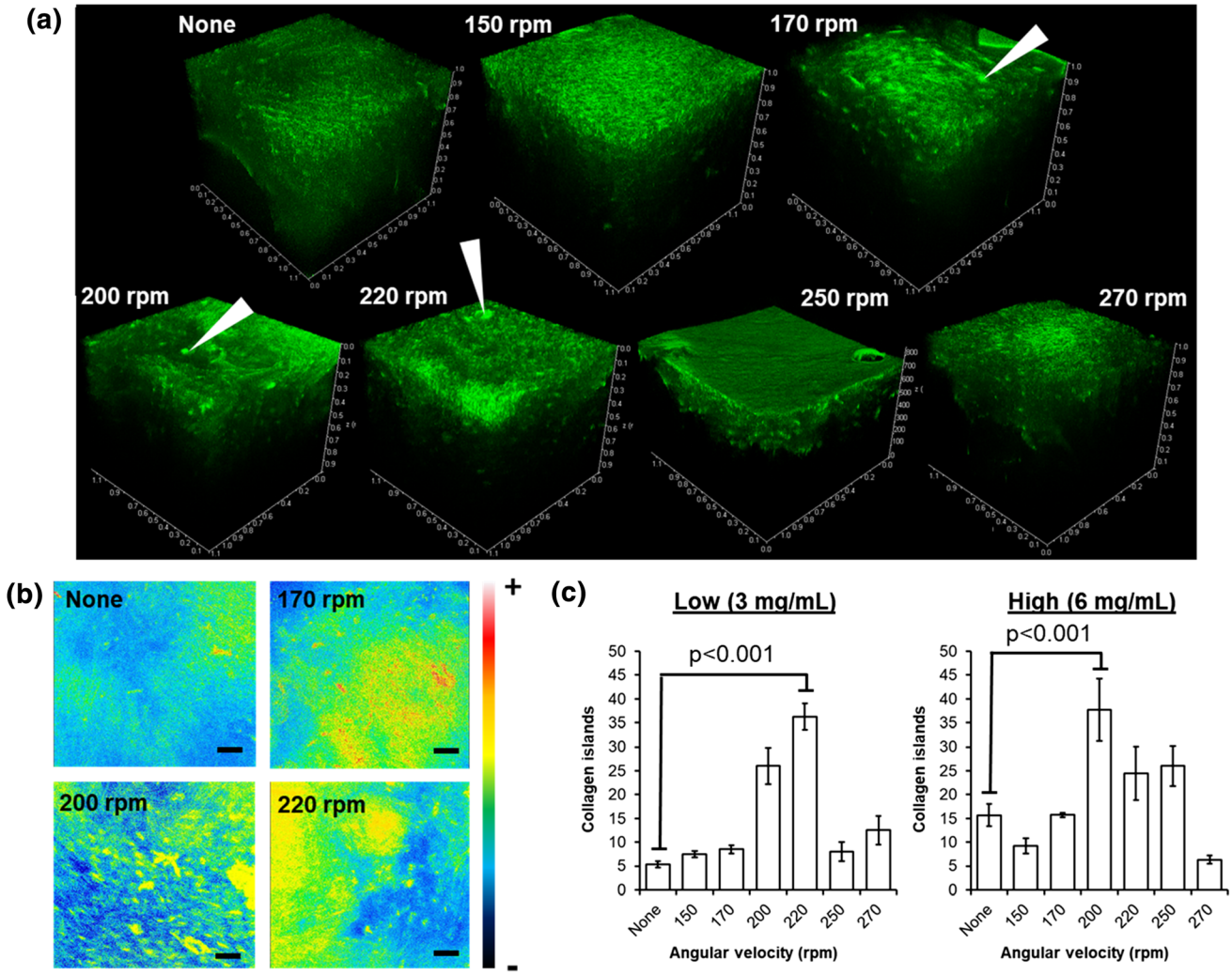

FIGURE 3. Collagen hydrogel deformation as a function of angular velocity. Reflectance imaging (green) *z*-stacks (1 mm^3) are displayed for each mechanical shaking condition (a). 3D re-constructions are presented with 0.1 mm increments along *x*, *y*, and *z* planes. Only examples of the 3 mg/mL collagen gel condition are presented; examples of collagen islands (hyperdensities) are indicated with white arrows (a). Heat maps of reflectance (white = most, black = least) highlight the spatial distribution of hyperdensities where punctate, island-like formations begin to emerge with exposures of 200 rpm (b, scale bars represent 50 μm). Collagen islands for Low (n = 4/group) and High (n = 4/group) concentration collagen conditions are quantified, revealing significantly increased values for angular velocities between 200 and 220 rpm relative to controls (None) (c). Means and standard error of the mean are provided with the most extreme differences indicated with p values ($p < 0.001$).

samples containing high concentration collagen (Fig. 3c). Together, these data indicated that mechanical shaking could deform collagen hydrogels, generating non-uniformities across the substrate.

Pre-shaken Collagen Substrates Increase Cell Death

As we predicted ECM deformation could affect cell viability and clustering behavior, 2D collagen surfaces were pre-exposed to the mechanical shaking paradigm and subsequently seeded with cortical monolayers. If the substrate was not a determinant of cell outcomes, different magnitudes of pre-shaking would generate the same outcomes. However, quantities of imaged dead cell as inferred by PI-positive signal increased linearly as a function of pre-exposure angular velocity (Figs. 4a and 4b, $r = 0.78$, $p < 0.05$) even though cells were never directly mechanically perturbed. Interneuronal space increased for 150, 170, 200, 220, and 250 rpm conditions relative to non-shaken controls; however, the 270 rpm condition displayed decreased interneuronal space ($p < 0.05$). Images of live cells revealed that despite generating increased PI-positive cells, the 270 rpm condition generated particularly large clusters of cells compared to all other conditions ($p < 0.001$, Figs. 4c and 4d). Similar to observations reported for 3D samples, 2D substrates displayed regions of torn collagen substrate which were infiltrated by clusters of cells with a high affinity for edges (Fig. 4c). To confirm the hypothesis that local collagen densities impacted cell attachment and clustering behaviour, drops of 6 mg/mL collagen were extruded over 3 mg/mL background within a 35 mm dish and later seeded with cells (density of 1.8×10^5 cells/cm^2). The drops, which simulated artificial, high-concentration collagen islands, ultimately became occupied by clusters of cells which were not observed on 3 mg/mL drops or on the neighboring 3 mg/mL background substrate (Figs. 5a and 5b). These data demonstrated that spatial inhomogeneities could precede and determine cell clustering behaviour and cell death.

ECM Deformation in Mechanically Shaken Neonatal Rat Brains

To verify that the applied forces associated with the mechanical shaking paradigm could realistically affect brain structure, experiments were carried out on post-

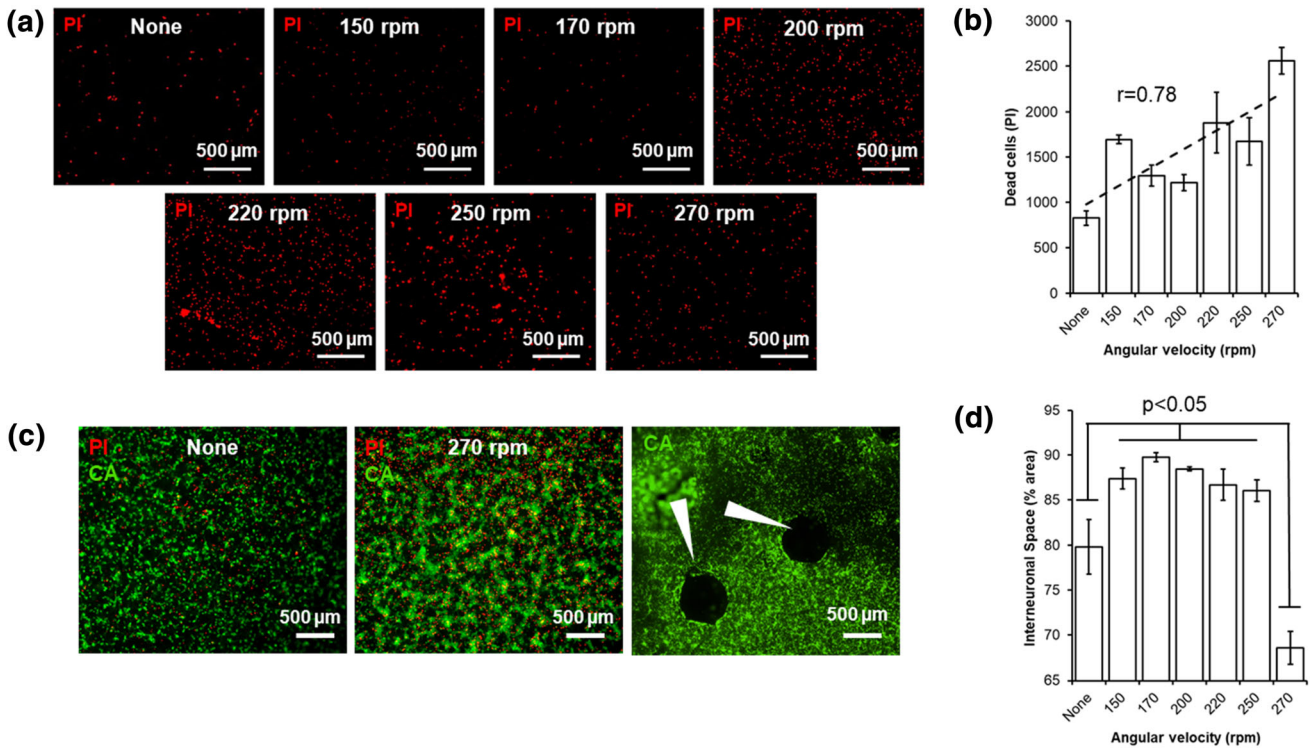

FIGURE 4. Pre-shaken 2D collagen substrates generate ECM deformations and increase cell death. PI-positive bodies indicative of cell death (a, red) increased linearly ($r = 0.78$; $n = 3$/condition) as a function of angular velocity associated with mechanical shaking of collagen substrates that were eventually seeded with rat cortical cells (b). Increased clustering (CA, green clusters) and cell death (PI, red bodies) were observed with increased shaking relative to controls with indications of collagen gel deformation (c, white arrows). Interneuronal space is also reported for each condition (d). Several significant differences were evident between conditions ($n = 3$/condition); three homogeneous subsets are indicated ($p < 0.05$). Means and standard error of the mean are provided. Scale bars are indicated.

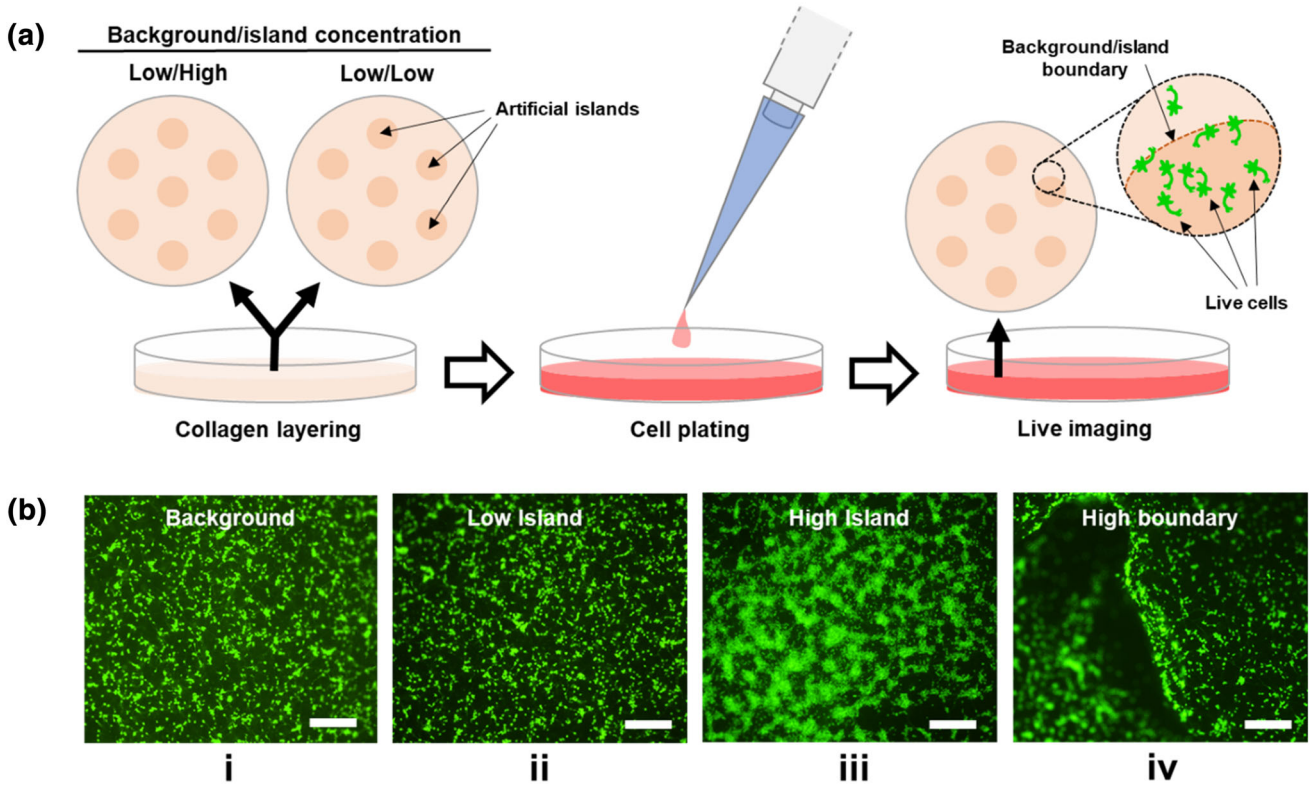

FIGURE 5. Artificial collagen islands induce concentration-dependent cell clustering. 35 mm dishes were covered with low-concentration (3 mg/mL) collagen gels (background) and later, drops (islands) of Low (3 mg/mL) or High (6 mg/mL) concentration collagen were deposited over the substrate (a). Cells were then seeded over the background/island landscapes and subject to live imaging. Live cell imaging (b, CA, green) revealed no cell clustering when low-concentration islands were placed over low concentration backgrounds (ii). However, when high-concentration islands were placed over low concentration backgrounds (iii), clustering occurred. A background-island boundary is also provided (iv), showing edge-effects. Scale bars represent 200 μm increments.

mortem neonatal rat brains. ECM deformation within neonatal brains exposed to the mechanical shaking paradigm was quantified by comparing the average fluorescent intensity of tissue subsections stained with anti-chondroitin sulfate antibodies. Mean gray values (MGVs) across tissue subsections represented averaged measures of anti-CS-positive tissue and the neighboring, comparatively darkened spaces indicative of vacuoles or tears. Anti-CS-positive fluorescent intensities within the CA fields of the HB were equivalent across shaking conditions ($p > 0.05$), however, differences of averaged fluorescent intensity were evident when comparing layers I–V of the S1 cortical region across angular velocity conditions, $F(2,17) = 5.20$, $p < 0.02$, $\eta^2 = 0.41$. *Post-hoc* tests revealed the source of variance to be a significant reduction of anti-CS-positive fluorescence within the 270 rpm condition relative to the no shaking condition, $t(8) = 3.64$, $p < 0.01$ (Fig. 6). Similarly, a reduction of DAPI-positive signal was apparent in S1 regions only ($p < 0.05$), indicating a loss of cell bodies in the highest angular velocity condition (270 rpm). These results indicated that ECM structure was disrupted during high-intensity shaking, generating more non-anti-CS-positive spaces within superficial tissues of the cerebral cortices.

DISCUSSION

To engineer an *in vitro* system to examine the effects of rotational acceleration on neural tissues, we designed and tested an *in vitro* mechanical shaking paradigm. Once it was established that shaking could significantly impact culture integrity and cause live cell clustering, we explored the possibility that physical perturbations of the collagen hydrogel in the absence of cells could generate gel deformations which might in turn affect cells. Blank (cell-free) samples were exposed to various shaking conditions and imaged to detect densiometric changes to the gels. It was revealed that fragmentation could be elicited with shaking such that more regions of increased collagen density could be detected with increased angular velocities. We hypothesized that collagen deformation, simulating ECM deformation, could precede cell effects including

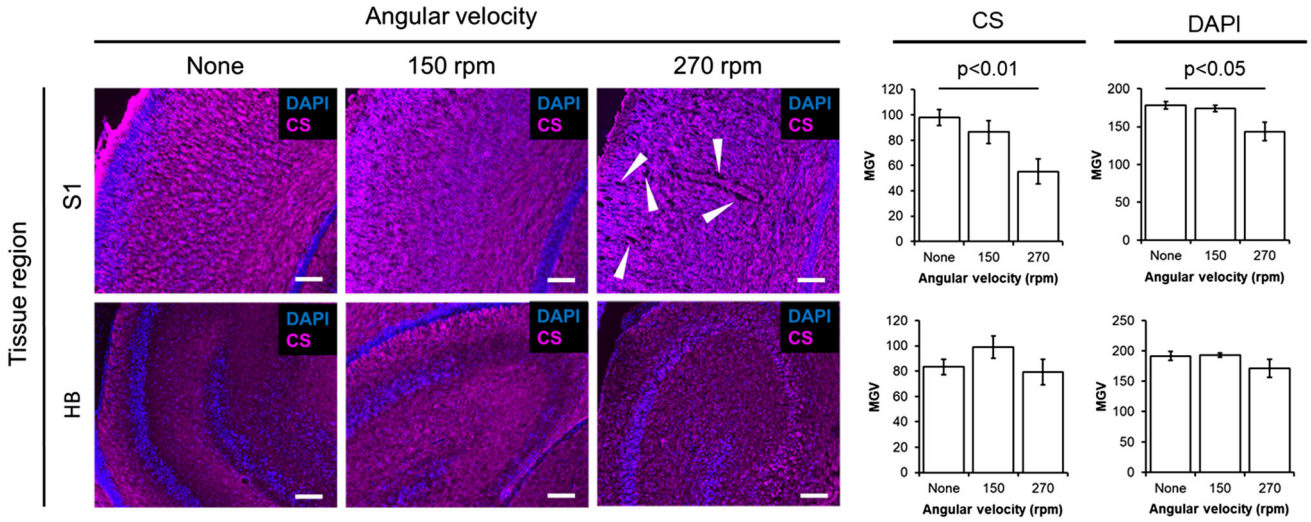

FIGURE 6. Neonatal rat brain ECM is deformed by mechanical shaking. S1 and HB tissue regions are displayed as a function of angular velocity conditions associated with mechanical shaking: None ($n = 5$), 150 rpm ($n = 8$), and 270 rpm ($n = 5$). Immunostained, chondroitin sulfate-positive (CS, magenta) sections are presented with counterstained cell nuclei (DAPI, blue). The cortical region, S1, exhibited increased vacuolization (white arrows) indicative of ECM tearing at 270 rpm relative to controls; quantification of fluorescent intensity (MGV) revealed a significant decrease in CS-positive fluorescence with increased angular velocity ($p < 0.01$). Similar decreases were observed for DAPI-positive staining in S1 sections ($p < 0.05$). Deep hippocampal body (HB) ECM was not affected by mechanical shaking, $p > 0.05$. Means and standard error of the means are provided. Scale bars indicate increments of 500 μm.

clustering and death. It was then confirmed that increased cell death and clustering could be elicited by pre-shaking two-dimensional collagen gel substrates before cell seeding. The same mechanical shaking paradigm could elicit ECM deformations and concomitant cell drop-out as inferred by decreased DAPI-positive signal which was limited to superficial tissue regions in post-mortem neonatal rat brains.

Our hypothesis that local changes to ECM structure could influence neural tissues is supported by previously reported findings. Matrix re-modelling enzymes were found to be secreted following cerebral ischemia and associated with neural progenitor cell migration.[37] Using collagen type-I as a substrate, Lo *et al.*[22] demonstrated "durotaxis"—a preference for stiff substrate—and dynamic responsiveness to applied strain in fibroblasts. Similar findings were reported in a bioengineered 3D brain tumor model.[36] Indeed, most investigations of ECM-neural interactions have focused on tumor processes[2,16,33] Considering mechanically deformed neurons increase excitotoxic,[29] glutamatergic signaling facilitated by *N*-methyl-D-aspartate (NMDA) receptors,[19] future studies should quantify the role of calcium on ECM deformation-mediated cell death. In particular, investigating the impacts of vibration, rotational acceleration, and microgravity on calcium-mediated secondary brain injuries resultant of brain ECM disruption would represent important milestones toward an understanding of subtle mechanical brain perturbations and their long-term consequences.

The 3D culture model presented here is an improvement over other 3D culture techniques including simple hydrogels as we are able to define spatial compartments within the construct (e.g., scaffold-region, central window, and lumen)—an essential feature when examining ectopic or migratory behavior. Importantly, as we have demonstrated that human cells can be cultured within the constructs for over 2 years,[28] the model system could serve as an investigative tool to evaluate the chronic effects of variable G-force exposure, sustained vibration, and microgravity associated with spaceflight and military aircraft operations. As suggested previously, evidence in support of model validity have been previously reported in populations of jet pilots and astronauts with WMHs.[1,20] *In vitro* systems such as the present 3D model of rotational acceleration represent important tools with which to investigate these possibilities as well as to screen interventions which might prevent or reverse their deleterious consequences.

ACKNOWLEDGMENTS

The authors would like to thank Martin Hunter, Will Collins, and Disha Sood for their technical expertise and assistance. This work was supported by the NIH (R01NS092847, P41EB027062, Research Infrastructure Grant NIHS10 OD021624).

REFERENCES

[1]Alperin, N., A. M. Bagci, and S. H. Lee. Spaceflight-induced changes in white matter hyperintensity burden in astronauts. *Neurology* 89(21):2187–2191, 2017.

[2]Ananthanarayanan, B., Y. Kim, and S. Kumar. Elucidating the mechanobiology of malignant brain tumors using a brain matrix-mimetic hyaluronic acid hydrogel platform. *Biomaterials* 32(31):7913–7923, 2011.

[3]Arenas, J. P., and R. N. Margasahayam. Noise and vibration of spacecraft structures. *Ingeniare. Revista chilena de ingeniería* 14(3):251–264, 2006.

[4]Cairns, D. M., K. Chwalek, Y. E. Moore, M. R. Kelley, R. D. Abbott, S. Moss, and D. L. Kaplan. Expandable and rapidly differentiating human induced neural stem cell lines for multiple tissue engineering applications. *Stem Cell Rep.* 7(3):557–570, 2016.

[5]Cantley, W. L., C. Du, S. Lomoio, T. DePalma, E. Peirent, D. Kleinknecht, *et al.* Functional and sustainable 3D human neural network models from pluripotent stem cells. *ACS Biomater. Sci. Eng.* 4(12):4278–4288, 2018.

[6]Chen, Y., and M. Ostoja-Starzewski. MRI-based finite element modeling of head trauma: spherically focusing shear waves. *Acta Mech.* 213(1–2):155–167, 2010.

[7]Chwalek, K., M. D. Tang-Schomer, F. G. Omenetto, and D. L. Kaplan. In vitro bioengineered model of cortical brain tissue. *Nat. Protoc.* 10(9):1362, 2015.

[8]Clayton, E. H., G. M. Genin, and P. V. Bayly. Transmission, attenuation and reflection of shear waves in the human brain. *J. R. Soc. Interface* 9(76):2899–2910, 2012.

[9]Cullen, D. K., M. C. Lessing, and M. C. LaPlaca. Collagen-dependent neurite outgrowth and response to dynamic deformation in three-dimensional neuronal cultures. *Ann. Biomed. Eng.* 35(5):835–846, 2007.

[10]George, N., and H. M. Geller. Extracellular matrix and traumatic brain injury. *J. Neurosci. Res.* 96(4):573–588, 2018.

[11]Giraudon, P., S. Buart, A. Bernard, N. Thomasset, and M. F. Belin. Extracellular matrix-remodeling metalloproteinases and infection of the central nervous system with retrovirus human T-lymphotropic virus type I (HTLV-I). *Prog. Neurobiol.* 49(2):169–184, 1996.

[12]Hayashi, T., Y. Kaneko, S. Yu, E. Bae, C. E. Stahl, T. Kawase, *et al.* Quantitative analyses of matrix metalloproteinase activity after traumatic brain injury in adult rats. *Brain Res.* 1280:172–177, 2009.

[13]Hirakawa, K., K. Hashizume, and T. Hayashi. Viscoelastic property of human brain-for the analysis of impact injury (author's transl). *No Shinkei* 33(10):1057–1065, 1981.

[14]Horner, P. J., and F. H. Gage. Regeneration in the adult and aging brain. *Arch. Neurol.* 59(11):1717–1720, 2002.

[15]Kartje-Tillotson, G., E. J. Neafsey, and A. J. Castro. Electrophysiological analysis of motor cortical plasticity after cortical lesions in newborn rats. *Brain Res.* 332(1):103–111, 1985.

[16]Kim, S. N., A. Jeibmann, K. Halama, H. T. Witte, M. Wälte, T. Matzat, *et al.* ECM stiffness regulates glial migration in Drosophila and mammalian glioma models. *Development* 141(16):3233–3242, 2014.

[17]Kiraly, M. A., and S. J. Kiraly. Traumatic brain injury and delayed sequelae: a review-traumatic brain injury and mild traumatic brain injury (concussion) are precursors to later-onset brain disorders, including early-onset dementia. *Sci. World J.* 7:1768–1776, 2007.

[18]Laksari, K., L. C. Wu, M. Kurt, C. Kuo, and D. C. Camarillo. Resonance of human brain under head acceleration. *J. R. Soc. Interface* 12(108):20150331, 2015.

[19]LaPlaca, M. C., and L. E. Thibault. Dynamic mechanical deformation of neurons triggers an acute calcium response and cell injury involving the N-methyl-D-aspartate glutamate receptor. *J. Neurosci. Res.* 52(2):220–229, 1998.

[20]Lee, J. K., V. Koppelmans, R. F. Riascos, K. M. Hasan, O. Pasternak, A. P. Mulavara, *et al.* Spaceflight-associated brain white matter microstructural changes and intracranial fluid redistribution. *JAMA Neurol.* 76(4):412–419, 2019.

[21]Lim, D., J. Park, W. H. Choi, D. H. Bang, O. M. Jung, and S. Kang. Asymptomatic brain lesions in pilots: a comparative study with non-flying personnel using brain MRI. *Aviat. Space Environ. Med.* 83(9):865–871, 2012.

[22]Lo, C. M., H. B. Wang, M. Dembo, and Y. L. Wang. Cell movement is guided by the rigidity of the substrate. *Biophys. J.* 79(1):144–152, 2000.

[23]Morris, R. G., J. Inglis, J. A. Ainge, H. J. Olverman, J. Tulloch, Y. Dudai, and P. A. Kelly. Memory reconsolidation: sensitivity of spatial memory to inhibition of protein synthesis in dorsal hippocampus during encoding and retrieval. *Neuron* 50(3):479–489, 2006.

[24]Muir, J., D. P. Kiel, and C. T. Rubin. Safety and severity of accelerations delivered from whole body vibration exercise devices to standing adults. *J. Sci. Med. Sport* 16(6):526–531, 2013.

[25]Oppenheimer, D. R. Microscopic lesions in the brain following head injury. *J. Neurol. Neurosurg. Psychiatry* 31(4):299, 1968.

[26]Paolicelli, R. C., G. Bolasco, F. Pagani, L. Maggi, M. Scianni, P. Panzanelli, *et al.* Synaptic pruning by microglia is necessary for normal brain development. *Science* 333(6048):1456–1458, 2011.

[27]Ribes, V., and J. Briscoe. Establishing and interpreting graded Sonic Hedgehog signaling during vertebrate neural tube patterning: the role of negative feedback. *Cold Spring Harbor Perspect. Biol.* 1(2):a002014, 2009.

[28]Rouleau, N., W. L. Cantley, V. Liaudanskaya, A. Berk, C. Du, W. Rusk, *et al.* A long-living bioengineered neural tissue platform to study neurodegeneration. *Macromol. Biosci.* 20:2000004, 2020.

[29]Siesjö, B. K., and P. Siesjö. Mechanisms of secondary brain injury. *Eur. J. Anaesthesiol.* 13(3):247–268, 1996.

[30]Sosa, M. A. G., R. De Gasperi, A. J. Paulino, P. E. Pricop, M. C. Shaughness, E. Maudlin-Jeronimo, *et al.* Blast overpressure induces shear-related injuries in the brain of rats exposed to a mild traumatic brain injury. *Acta Neuropathol. Commun.* 1(1):51, 2013.

[31]Spear, R. C., C. A. Keller, and T. H. Milby. Morbidity studies of workers exposed to whole body vibration. *Arch. Environ. Health* 31(3):141–145, 1976.

[32]Tang-Schomer, M. D., J. D. White, L. W. Tien, L. I. Schmitt, T. M. Valentin, D. J. Graziano, *et al.* Bioengineered functional brain-like cortical tissue. *Proc. Natl. Acad. Sci.* 111(38):13811–13816, 2014.

[33]Ulrich, T. A., E. M. de Juan Pardo, and S. Kumar. The mechanical rigidity of the extracellular matrix regulates the structure, motility, and proliferation of glioma cells. *Cancer Res.* 69(10):4167–4174, 2009.

[34]Urbán, N., and F. Guillemot. Neurogenesis in the embryonic and adult brain: same regulators, different roles. *Front. Cell. Neurosci.* 8:396, 2014.

[35]Wang, X., J. Jung, M. Asahi, W. Chwang, L. Russo, M. A. Moskowitz, *et al*. Effects of matrix metalloproteinase-9 gene knock-out on morphological and motor outcomes after traumatic brain injury. *J. Neurosci*. 20(18):7037–7042, 2000.

[36]Wang, C., X. Tong, and F. Yang. Bioengineered 3D brain tumor model to elucidate the effects of matrix stiffness on glioblastoma cell behavior using PEG-based hydrogels. *Mol. Pharm*. 11(7):2115–2125, 2014.

[37]Wang, L., Z. G. Zhang, R. L. Zhang, S. R. Gregg, A. Hozeska-Solgot, Y. LeTourneau, *et al*. Matrix metalloproteinase 2 (MMP2) and MMP9 secreted by erythropoietin-activated endothelial cells promote neural progenitor cell migration. *J. Neurosci*. 26(22):5996–6003, 2006.

[38]Wardlaw, J. M., M. C. Valdés Hernández, and S. Muñoz-Maniega. What are white matter hyperintensities made of? Relevance to vascular cognitive impairment. *J. Am. Heart Assoc*. 4(6):e001140, 2015.

[39]Yan, J. G., L. L. Zhang, M. Agresti, J. LoGiudice, J. R. Sanger, H. S. Matloub, and R. Havlik. Neural systemic impairment from whole-body vibration. *J. Neurosci. Res*. 93(5):736–744, 2015.

[40]Yan, J. G., L. L. Zhang, M. Agresti, Y. Yan, J. LoGiudice, J. R. Sanger, *et al*. Cumulative brain injury from motor vehicle-induced whole-body vibration and prevention by human apolipoprotein AI molecule mimetic (4F) peptide (an Apo AI mimetic). *J. Stroke Cerebrovasc. Dis*. 24(12):2759–2773, 2015.

[41]Zhao, B. Q., E. Tejima, and E. H. Lo. Neurovascular proteases in brain injury, hemorrhage and remodeling after stroke. *Stroke* 38(2):748–752, 2007.

Publisher's Note Springer Nature remains neutral with regard to jurisdictional claims in published maps and institutional affiliations.